

Mask-free construction of three-dimensional silicon structures by dry etching assisted gray-scale femtosecond laser direct writing

Xue-Qing Liu, Lei Yu, Qi-Dai Chen, and Hong-Bo Sun

Citation: *Appl. Phys. Lett.* **110**, 091602 (2017); doi: 10.1063/1.4977562

View online: <http://dx.doi.org/10.1063/1.4977562>

View Table of Contents: <http://aip.scitation.org/toc/apl/110/9>

Published by the [American Institute of Physics](#)

Articles you may be interested in

[Shape formation of helical ribbons induced by material anisotropy](#)

Appl. Phys. Lett. **110**, 091901091901 (2017); 10.1063/1.4977090

[How predictable is plastic damage at the atomic scale?](#)

Appl. Phys. Lett. **110**, 091902091902 (2017); 10.1063/1.4977420

[Optical investigation of semi-polar \(11-22\) Al_xGa_{1-x}N with high Al composition](#)

Appl. Phys. Lett. **110**, 091102091102 (2017); 10.1063/1.4977428

[Optofluidic Fano resonance photonic crystal refractometric sensors](#)

Appl. Phys. Lett. **110**, 091105091105 (2017); 10.1063/1.4977563



Small Conferences. BIG Ideas.

Applied Physics
Reviews

SAVE THE DATE!
3D Bioprinting: Physical and Chemical Processes
May 2–3, 2017 • Winston Salem, NC, USA

Mask-free construction of three-dimensional silicon structures by dry etching assisted gray-scale femtosecond laser direct writing

Xue-Qing Liu,¹ Lei Yu,¹ Qi-Dai Chen,^{1,a)} and Hong-Bo Sun^{1,2,a)}

¹State Key Laboratory on Integrated Optoelectronics, College of Electronic Science and Engineering, Jilin University, 2699 Qianjin Street, Changchun 130012, People's Republic of China

²College of Physics, Jilin University, 2699 Qianjin Street, Changchun 130012, People's Republic of China

(Received 12 December 2016; accepted 14 February 2017; published online 2 March 2017)

A mask-free micro/nano fabrication method is proposed for constructing arbitrary gradient height structures on silicon, combining gray-scale femtosecond laser direct writing (GS-FsLDW) with subsequent dry etching. Arbitrary two-dimensional patterns with a gradient concentration of oxygen atoms can be fabricated on the surface of undoped silicon wafer by FsLDW in air. After dry etching, various three-dimensional (3D) gradient height silicon structures are fabricated by controlling the laser power, scanning step, etching time, and etching power. As an example, a well-defined 3D Fresnel zone plate was fabricated on silicon wafer, which shows excellent focusing and imaging properties. The combination of high precision from dry etching and 3D fabrication ability on non-planar substrates of FsLDW, may broaden its applications in microelectronics, micro-optics, and microelectromechanical systems. *Published by AIP Publishing.* [<http://dx.doi.org/10.1063/1.4977562>]

Silicon micro/nano structures have attracted attention in recent years due to their wide application in electronics,¹ photoelectronic devices,^{2,3} biosensors,⁴ and micro/nano-electromechanical systems (M/NEMS).⁵ A widely used method for fabricating silicon structures is photolithography combined with etching, and this is convenient for constructing planar structures. Although three-dimensional (3D) structures can be fabricated by multiple photolithography and etching steps, the morphology profile of the structures is limited to step structures. Therefore, various 3D fabrication methods have been developed to fabricate the arbitrary gradient height structures or 3D structures on various materials.^{6–11} Among these fabrication strategies, due to its compatibility with the integrated circuit (IC) process and the controllable profiles that can be obtained with a proper mask, gray-scale photolithography has been demonstrated as an effective method for constructing the gradient height silicon structures via one step photolithography followed by dry etching.^{11–17} Microfluidic structures,¹⁸ refractive microlenses¹⁴ and micro-compressors¹³ which have been realized by gray-scale photolithography technology, are widely used in lab on a chip systems, micro-optics, and MEMS, respectively. However, shortcomings also exist when fabricating complex structures by the gray-scale photolithography technology, e.g., the fabrication of gray-scale masks always require multiple complex procedures.¹⁶ These masks are expensive, and structures can only be fabricated on planar substrates. Therefore, there is an urgent need for novel flexible mask-free micro/nano 3D fabrication methods to construct arbitrary gradient height structures on silicon.

As a mask-free micro/nano fabrication technology, femtosecond laser direct writing (FsLDW) has been widely used to fabricate 3D structures for various materials.^{19–25} However, most of the explorations on micromachining of semiconductors or metals using femtosecond laser are focused on their

surfaces.^{26,27} This is because not only are these materials opaque to the 800 nm femtosecond laser light, but it is also time-consuming to directly construct 3D structures on the substrates by such a point by point fabrication method. Here, a mask-free micro/nano fabrication method is proposed for constructing arbitrary gradient height structures on silicon. This method combines gray-scale FsLDW with subsequent dry etching. The gray-scale FsLDW technology has been proposed as a mean of fabricating continuous-tone gray-scale photomasks,²⁸ where the gray-scale information can be flexibly recorded in materials (depending on the laser power). Based on this technology, arbitrary two-dimensional (2D) patterns with a gradient concentration of oxygen atoms were fabricated on the surface of undoped silicon wafer by gray-scale FsLDW in air. Then, the patterned silicon wafer was etched using a SF₆ plasma in an inductively coupled plasma (ICP) system for fabricating arbitrary gradient height 3D silicon structures without any additional photolithography process. As the etching rates for regions with different concentrations of oxygen atoms are different, arbitrary programmable 3D structures on silicon can be flexibly fabricated by dry-etching assisted gray-scale FsLDW.

The dry etching assisted gray-scale FsLDW technology contained two steps for fabricating gradient height structures on silicon, as shown by the schematic diagram in Fig. 1. First, arbitrary programmable 2D patterns can be flexibly fabricated on the surface of undoped silicon wafer by FsLDW. Here, the silicon atoms can be oxidized in the laser irradiated region during the process of laser patterning. Furthermore, the mean concentration of oxygen atoms can be adjusted by controlling the energy density of the laser power. Thus, 2D structures with gray-scale gradient concentrations of oxygen atoms can be formed on silicon wafer. Then, the patterned silicon wafer can be etched by a SF₆ plasma in an ICP system. The etching rates would be different between the unmodified and laser treated regions. In addition, the etching rates would vary with different concentrations of oxygen atoms. As the etching rate

^{a)}Authors to whom correspondence should be addressed. Electronic mail: chenqd@jlu.edu.cn and hbsun@jlu.edu.cn

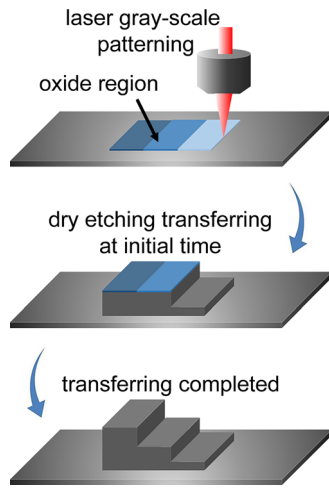


FIG. 1. Schematic diagram of the dry etching assisted gray-scale femtosecond laser direct writing process. First, 2D patterns can be flexibly fabricated on the surface of the undoped silicon wafer by FsLDW. Then, 3D gradient height structures can be fabricated after dry etching.

of silicon dioxide (100 nm/min) is slower than that of silicon (1000 nm/min) when etched by fluorine-based gas,^{29,30} the height of the laser patterned areas would be higher than the unmodified regions. Therefore, gradient height structures could be fabricated by controlling the concentration of oxygen atoms affected by the mean laser power density in the patterns. Although the chemical wet etching has been used for transferring 2D patterns,³¹ the distortion of designed structures would be caused by serious lateral etching and crystal-orientation-based etching. What is more, gray-scale 3D structures are difficult to be realized by wet etching. Gray-scale 2D patterns can be transferred to 3D structures through ICP etching, by which the etching rate of the lateral and longitudinal etching can be controlled via an appropriate radio frequency (RF) power of the bottom electrode.

As shown in Fig. 2(a), a series of square patterns were fabricated by FsLDW with different scanning steps. The power of the laser pulse was 120 mW. The mean energy density of laser power printed on the surface of silicon wafer is related to the scanning steps. With an increase in the scanning steps from 50 nm to 1 μm , the extent of interaction between laser pulses and silicon wafer decreased. To understand the influence of the laser pulse on silicon, energy dispersive spectroscopy (EDS) was adopted to analyze the contained elements of laser patterned regions (as shown in Fig. S1 of [supplementary material](#)). It indicates that parts of silicon atoms can be oxidized in laser irradiated regions, as the oxygen element map shows in Fig. 2(b). It has been demonstrated that silicon can be oxidized with the crystal structure transforming from crystalline to amorphous in the modified regions after laser irradiation.³² The presence of dangling bonds and the local heating effect related to the instantaneous accumulation of laser energy and high absorption may contribute to the oxygen incorporation.³³ With an increase in the scanning steps, the mean energy density of laser power that was printed on the surface of the silicon wafer decreased, as shown in Fig. 2(c).

Then, the patterned silicon wafer was etched by SF_6 plasma for 10 min. As the etching rate of silicon dioxide is slower than

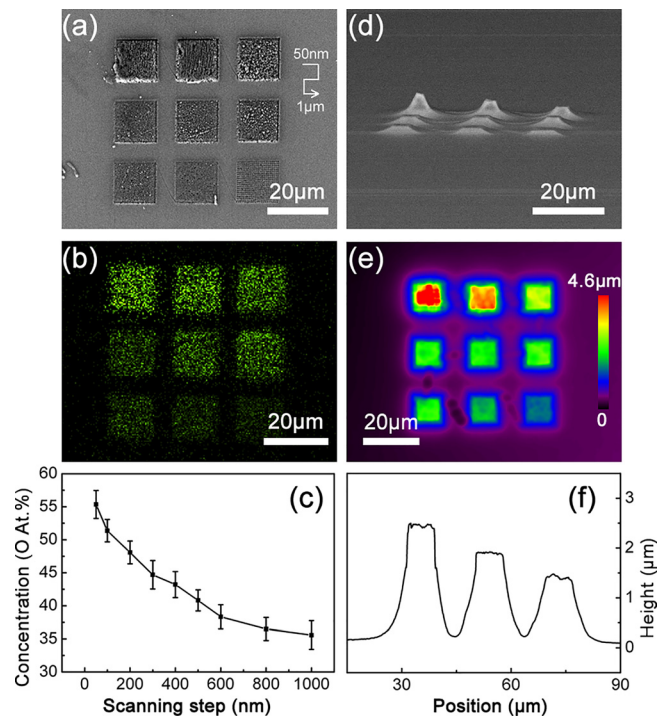


FIG. 2. (a) SEM images of square patterns fabricated by FsLDW with scanning steps of 50, 100, 200, 300, 400, 500, 600, 800, and 1000 nm. (b) Oxygen map obtained by EDS corresponding to square patterns in (a). (c) The relationship of concentration of oxygen atoms in laser modified regions with scanning steps. (d) SEM images of square steps after etching for 10 min. (e) and (f) are photos according to height information and cross-section profiles obtained using CLSM.

that of silicon when etched by fluorine-based gas, the height of laser patterned areas would be higher than that of the unmodified regions, which is exhibited in Fig. 2(d). The height of the structures after etching increased with an increase in the concentration of oxygen atoms. Thus, this also indicates that the height of structures after etching can increase with a decrease in the scanning step. To further prove this phenomenon, the height of the silicon structures was also measured by confocal laser scanning microscopy (CLSM). Photos according to height information and cross-section profiles obtained using CLSM are shown in Figs. 2(e) and 2(f), respectively. According to Fig. 2(f), distinct height steps can be formed by this dry etching assisted gray-scale FsLDW technology. Surface smoothness is crucial for microstructures to be applied in optical devices. Therefore, surface roughness defined by the root-mean-square (RMS) of a polished silicon wafer, a laser structured silicon surface, a polished silicon wafer after etching for 10 min, and a laser structured silicon surface after etching for 10 min were measured by atomic force microscopy (AFM), as shown in Fig. S2 ([supplementary material](#)). The surface roughness values are 0.1, 103, 0.3, and 22.3 nm, respectively. Notably, compared with the laser structured wafer, the surface roughness of laser structured silicon after etching decreases to 20 nm. It might, therefore, be concluded that surface smoothness of laser structured wafer can be improved using a dry etching process.

From the above, it can be concluded that the concentration of oxygen atoms is related to the mean energy density of laser power printed on the surface of silicon wafer. Therefore, the height of structures after etching can be adjusted by controlling the mean energy density of laser power printed on the surface

of silicon wafer. Here, two ways can be adopted to change the mean energy density of laser power printed on the surface of silicon wafer: the power of the laser pulse and scanning steps. To investigate the dependence of the heights of the silicon structures formed after etching on the laser power, a series of square patterns were fabricated on silicon wafer by FsLDW with a laser power ranging from 50 to 250 mW and scanning step of 200 nm. Then, the above sample was etched for 10 min by SF_6 in the ICP. As shown in Fig. 3(a), the height of the structures increases approximately linearly with an increase in laser power. It is well known that the accumulated amounts of laser pulses would be affected by the scanning steps during the laser process. Therefore, the mean energy density of laser power printed on the surface of silicon wafer can be adjusted by adjusting the scanning steps. Fig. 3(b) exhibits the evolution of the height of silicon structures as a function of scanning steps. With a laser power of 120 mW, the range of scanning step was controlled from 50 nm to 1 μm , and the etching time was 10 min. The results demonstrate that the height of the structures decreased approximately as the inverse square of the scanning step. This is because the mean energy density of laser power printed on the surface of silicon wafer decreases as the inverse square of the scanning step.

Except for the laser power and scanning step, the height of the structures is also affected by the etching process. Fig. 3(c) shows the relationship between the height of the silicon structures and etching time. The laser power was 120 mW, and the scanning step was 200 nm. The height of the silicon structures increased to a maximum value after the initial several minutes of etching, demonstrating that the etching rate of the laser modified region is lower than that of the untreated silicon during the initial etching procedure. As the oxide layer is completely etched, the height of the silicon structures gradually stabilized to a value with a further increase in etching time. Another important factor that influences the height of these structures is the bottom electrode RF power of the ICP system. For ICP etching, both chemical reactive etching and physical bombardment exist during the etching process. The physical bombardment

etching rate can be enhanced by increasing the bias of the bottom electrode. As shown in Fig. 3(d), the height of the silicon structures decreased with an increase in the bias of the bottom electrode. The results indicate that the difference in etching rate between the modified and untreated regions can be reduced by increasing the bias of the bottom electrode.

As the concentration of oxygen atoms can be adjusted by the laser power and scanning steps, arbitrary programmable 2D patterns can be flexibly fabricated on the surface of undoped silicon wafer by this gray-scale FsLDW approach. After etching, the gradient height of 3D structures would be fabricated according to the 2D patterns. As the SEM image shows in Fig. 4(a), three-level steps are realized by controlling the scanning step. In addition, more complex structures, such as the word "LASER" on a rectangular step, can be fabricated by pre-designing the 2D pattern, as shown in Fig. 4(b). Not only step-like structures, but also continuous variable height structures can be formed by this dry etching assisted gray-scale FsLDW technology. For example, a rectangular pyramid and focal varying concave microlens array were fabricated on the surface of silicon, as shown in Figs. 4(c) and 4(d). It is demonstrated that arbitrary gradient 3D silicon structures can be fabricated by dry etching assisted gray-scale FsLDW technology. The height information photos and cross-section profiles are shown in Figs. S3 and S4 (supplementary material).

To verify the technical feasibility of fabricating arbitrary gradient 3D silicon structures on silicon wafer with step-like structures and continuous variable height structures on the same sample, a Fresnel zone plate (FZP) was designed and fabricated. Fig. 5(a) shows the SEM image of a 2D FZP pattern on the surface of silicon fabricated by gray-scale FsLDW without etching. Then, the pattern was transferred to silicon by etching for 6 min. The SEM image is shown in Fig. 5(b). The 3D morphology and cross-section profile were investigated and characterized by CLSM, as shown in Figs. 5(c) and 5(d). The height of the fabricated FZP is about 3.2 μm (Fig. 5(d)). The fabricated silicon FZP exhibited not only an excellent surface quality but also well-defined geometry. The reflected imaging system was adopted for characterizing the focusing

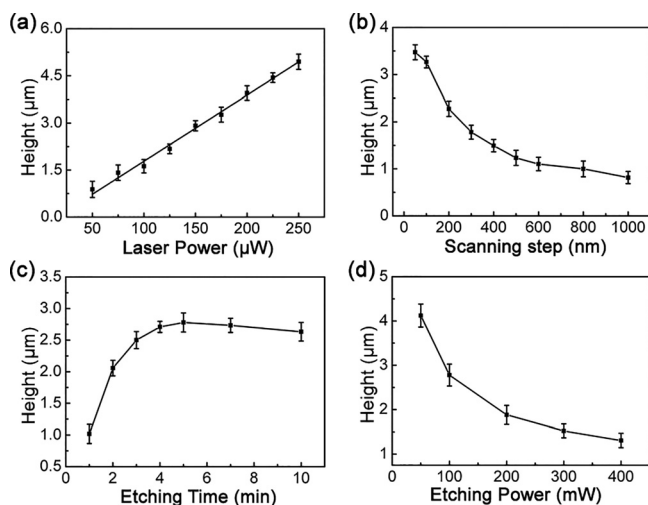


FIG. 3. The relationship of the height of structures after etching with laser power (a), scanning steps (b), etching time (c), and the bottom electrode radio-frequency (RF) power (d).

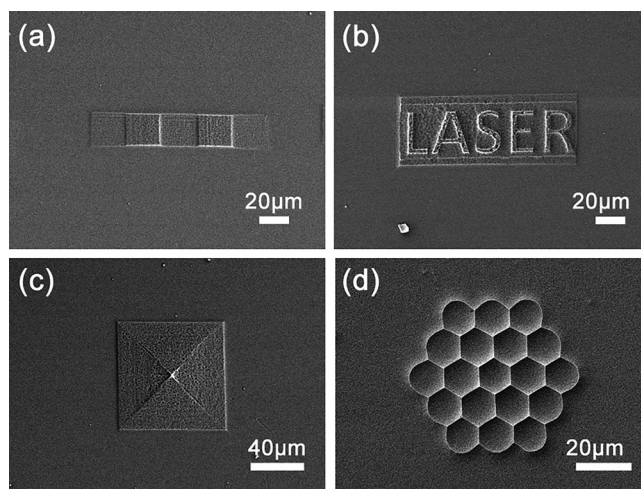


FIG. 4. SEM images of three-level steps (a), the word "LASER" on a rectangular step (b), rectangular pyramid (c) and focal varying concave microlens array (d) are fabricated on the surface of silicon.

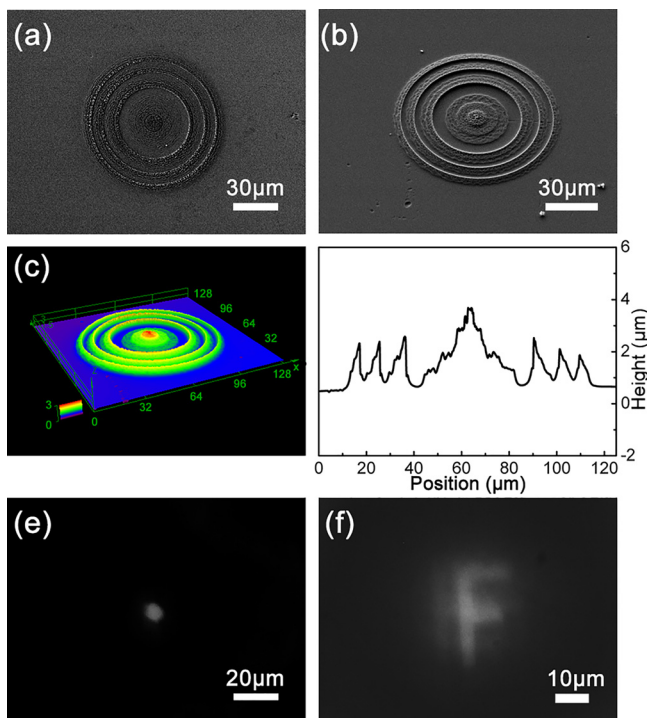


FIG. 5. SEM images of FZP fabricated before (a) and after (b) etching for 6 min. (c) and (d) are the 3D morphology and cross-section profile characterized by CLSM, respectively. (e) and (f) are photo images of the focal spot and imaging of letter “F” obtained by silicon FZP.

and imaging performance of the silicon FZP. The size of the focal spot was measured to be approximately $8 \mu\text{m}$, as shown in Fig. 5(e). Moreover, the image of the letter “F” can be clearly observed using a charge coupled device camera, as shown in Fig. 5(f). From the above, a well-defined 3D FZP can be fabricated by dry etching assisted gray-scale FsLDW, which shows excellent focusing and imaging properties.

In conclusion, a mask-free micro/nano fabrication method, termed dry etching assisted gray-scale femtosecond laser direct writing (GS-FsLDW), is proposed for constructing arbitrary gradient height structures on silicon. The height of the silicon structures can be flexibly adjusted by controlling the laser power, scanning step, etching time, and the bottom electrode RF power. Various complex 3D structures can be realized on the surface of silicon wafer. The method is expected to be able to solve the complexity of traditional lithography and common difficulties of FsLDW when fabricating gradient 3D structures on silicon wafer. Although only silicon structures are fabricated in this work, we believe that various materials could be used to fabricate flexible structures by inducing differences in etching rates by FsLDW. The combination of high precision of dry etching and 3D fabrication ability on non-planar substrates by FsLDW,³⁴ may broaden its application in microelectronics, micro-optics, and MEMS.

See [supplementary material](#) for the following information: Energy dispersive spectroscopy (EDS) is adopted to analyze the contained elements of laser patterned regions. RMS of a polished silicon wafer, a laser structured silicon surface, a polished silicon wafer after etching for 10 min, and a laser structured silicon surface after etching for 10 min

are measured by AFM. The height information photos and the cross-section profiles are obtained by LSCM.

The authors acknowledge the supports from National Science Foundation of China (NSFC) under Grant Nos. 91423102, 91323301, 51335008 and 61590930, and National Basic Research Program of China (973 program) under Grant No. 2014CB921302.

- ¹L. Sainiemi, V. Jokinen, A. Shah, M. Shpak, S. Aura, P. Suvanto, and S. Franssila, *Adv. Mater.* **23**, 122–126 (2011).
- ²X. Wu, X. Pan, B. Quan, and L. Wang, *Appl. Phys. Lett.* **103**, 121112 (2013).
- ³F. Priolo, T. Gregorkiewicz, M. Galli, and T. F. Krauss, *Nat. Nanotechnol.* **9**, 19–32 (2014).
- ⁴J. D. Ryckman, M. Liscidini, J. E. Sipe, and S. M. Weiss, *Appl. Phys. Lett.* **96**, 171103 (2010).
- ⁵S.-m. Sim, Y. Lee, Y.-H. Jang, Y.-S. Lee, Y.-K. Kim, I. Llamas-Garro, and J.-M. Kim, *Microelectron. Eng.* **162**, 69 (2016).
- ⁶B. Quan, Z. Yao, W. Sun, Z. Liu, X. Xia, C. Gu, and J. Li, *Microelectron. Eng.* **163**, 110 (2016).
- ⁷S. Azimi, M. B. H. Breese, Z. Y. Dang, Y. Yan, Y. S. Ow, and A. A. Bettiol, *J. Micromech. Microeng.* **22**, 015015 (2012).
- ⁸S. Azimi, J. Song, Z. Y. Dang, H. D. Liang, and M. B. H. Breese, *J. Micromech. Microeng.* **22**, 113001 (2012).
- ⁹K. Kashyap, A. Kumar, C.-T. Huang, Y.-Y. Lin, M. T. Hou, and J. A. Yeh, *Sci. Rep.* **5**, 10869 (2015).
- ¹⁰Z. Yin, L. Qi, H. Zou, and L. Sun, *Sci. Rep.* **6**, 18921 (2016).
- ¹¹J. D. Rogers, A. H. O. Kärkkäinen, T. Tkaczyk, J. T. Rantala, and M. R. Descour, *Opt. Express* **12**, 1294 (2004).
- ¹²C. F. Chen, S. D. Tzeng, H. Y. Chen, and S. Gwo, *Opt. Lett.* **30**, 652 (2005).
- ¹³C. M. Waits, B. Morgan, M. Kastantin, and R. Ghodssi, *Sens. Actuators, A* **119**, 245 (2005).
- ¹⁴C.-C. Chen, M.-H. Li, C.-Y. Chang, J.-K. Sheu, G.-C. Chi, W.-T. Cheng, J.-H. Yeh, J.-Y. Chang, and T. Ito, *Opt. Commun.* **215**, 75 (2003).
- ¹⁵M. W. Christopher, M. Alireza, and G. Reza, *J. Micromech. Microeng.* **13**, 170 (2003).
- ¹⁶Y. Pang, Y. Shu, M. Shavezipur, X. Wang, M. A. Mohammad, Y. Yang, H. Zhao, N. Deng, R. Maboudian, and T.-L. Ren, *Sci. Rep.* **6**, 28552 (2016).
- ¹⁷L. Li, Y. Liu, X. Zhao, Z. Lin, and C.-P. Wong, *ACS Appl. Mater. Interfaces* **6**, 575 (2014).
- ¹⁸J. Atencia, S. Barnes, J. Douglas, M. Meacham, and L. E. Locascio, *Lab Chip* **7**, 1567 (2007).
- ¹⁹F. Chen, D. Zhang, Q. Yang, J. Yong, G. Du, J. Si, F. Yun, and X. Hou, *ACS Appl. Mater. Interfaces* **5**, 6777 (2013).
- ²⁰K.-S. Lee, R. H. Kim, D.-Y. Yang, and S. H. Park, *Prog. Polym. Sci.* **33**, 631 (2008).
- ²¹K. Sugioka and Y. Cheng, *Light Sci. Appl.* **3**, e149 (2014).
- ²²M. D. Turner, M. Saba, Q. Zhang, B. P. Cumming, G. E. Schroder-Turk, and M. Gu, *Nat. Photonics* **7**, 801 (2013).
- ²³D. Wu, J. Xu, L.-G. Niu, S.-Z. Wu, K. Midorikawa, and K. Sugioka, *Light Sci. Appl.* **4**, e228 (2015).
- ²⁴J. Zhang, R. Drevinskis, M. Beresna, and P. G. Kazansky, *Appl. Phys. Lett.* **107**, 041114 (2015).
- ²⁵Q. Sun, F. Liang, R. Vallée, and S. L. Chin, *Opt. Lett.* **33**, 2713 (2008).
- ²⁶T. Y. Hwang and C. Guo, *Opt. Lett.* **36**, 2575 (2011).
- ²⁷K. K. Anoop, A. Rubano, R. Fittipaldi, X. Wang, D. Paparo, A. Vecchione, L. Marrucci, R. Bruzzese, and S. Amoroso, *Appl. Phys. Lett.* **104**, 241604 (2014).
- ²⁸C. F. Guo, S. Cao, P. Jiang, Y. Fang, J. Zhang, Y. Fan, Y. Wang, W. Xu, Z. Zhao, and Q. Liu, *Opt. Express* **17**, 19981 (2009).
- ²⁹L. Lallement, C. Gosse, C. Cardinaud, M.-C. Peignon-Fernandez, and A. Rhallabi, *J. Vac. Sci. Technol., A* **28**, 277 (2010).
- ³⁰S. Gomez, R. Jun Belen, M. Kiehlauch, and E. S. Aydil, *J. Vac. Sci. Technol., A* **22**, 606 (2004).
- ³¹A. Kiani, K. Venkatakrishnan, B. Tan, and V. Venkataramanan, *Opt. Express* **19**, 10834 (2011).
- ³²M. J. Smith, M.-J. Sher, B. Franta, Y.-T. Lin, E. Mazur, and S. Gradečak, *J. Appl. Phys.* **112**, 083518 (2012).
- ³³A. Pan, J. Si, T. Chen, Y. Ma, F. Chen, and X. Hou, *Opt. Express* **21**, 16657 (2013).
- ³⁴B.-B. Xu, H. Xia, L.-G. Niu, Y.-L. Zhang, K. Sun, Q.-D. Chen, Y. Xu, Z.-Q. Lv, Z.-H. Li, H. Misawa, and H.-B. Sun, *Small* **6**, 1762 (2010).